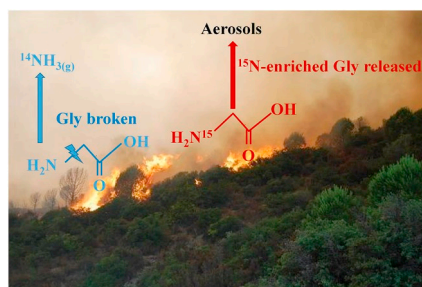# Nitrogen isotopic composition of free Gly in aerosols at a forest site

Ren-guo Zhu [a,b], Hua-Yun Xiao [a,b,*], Zhe Lv [a], Hao Xiao [b], Zhongyi Zhang [a], Nengjian zheng [a], Hongwei Xiao [a,**]

[a] *Jiangxi Province Key Laboratory of the Causes and Control of Atmospheric Pollution, East China University of Technology, Nanchang, 330013, China*
[b] *State Key Laboratory of Environmental Geochemistry, Institute of Geochemistry, Chinese Academy of Sciences, Guiyang, 550081, China*

HIGHLIGHTS

- Nitrogen isotope of free Gly in total suspended particulates were first reported.
- Nitrogen isotope of free Gly in aerosol might be useful for tracing biomass burning.
- Bituminous combustion and vehicle emissions may not be the source of free Gly.

GRAPHICAL ABSTRACT

ARTICLE INFO

ABSTRACT

The nitrogen isotope composition of free glycine ($\delta^{15}N_{F-Gly}$) in atmospheric particulates from different sources was measured to explore whether $\delta^{15}N_{F-Gly}$ could be used to indicate the sources of particulates. We found that the $\delta^{15}N_{F-Gly}$ released by biomass combustion (range: +16.9 to +27.3‰) was significantly higher than that from natural sources (up to 21.6‰). The concentration of free Gly in particulates released from fossil fuel combustion (bituminite combustion and vehicle emission) was very low. These results provided the possibility for using the $\delta^{15}N_{F-Gly}$ values in aerosol to distinguish biomass combustion from natural sources. In the field, a high correlation between the free Gly concentrations in aerosol and nonsea salt potassium (nss-K^+) was observed. The $\delta^{15}N_{F-Gly}$ values showed the same temporal pattern with fire points and a link between the $\delta^{15}N_{F-Gly}$ values and nss-K^+ levels was found. These results suggested that the $\delta^{15}N_{F-Gly}$ value in aerosol might be a good indicator for biomass burning.

1. Introduction

As an important source of atmospheric particulate matter (PM), biomass burning may contribute more than 45% to the total PM concentration during heavy pollution days (Qiu et al., 2016). Additionally, biomass burning discharges a large amount of PM composed of nitrogen (N)-containing organic compounds, oxidized organic carbon and black carbon or soot, which could have significant climate implications and may cause deleterious effects on human health (Fu et al., 2012; Zhang et al., 2011). Therefore, numerous studies have resorted to investigating

ARTICLE IN PRESS

R.-g. Zhu et al.   Atmospheric Environment xxx (xxxx) xxx

molecules markers (e.g., levoglucosan, potassium, etc.) as a versatile tool to indicate biomass burning (Cheng et al., 2013; Feng et al., 2006; Salma et al., 2017). However, it was recently demonstrated that levoglucosan reacts with OH radicals, with an atmospheric half-life of a few days (Hennigan et al., 2010). The sources of the potassium ion (K^+) are complex and include biomass burning, sea salt, crustal materials, and fireworks (Harrison et al., 2012). Consequently, these factors may cause large uncertainties in source apportionment. There is an urgent need for introducing other tracers to improve biomass burning source apportionment.

Because stable N isotope composition ($\delta^{15}N$) value can hold source-specific information, it has become a unique and effective tool to identify potential sources of the dominant N compounds in the atmosphere (Xiao et al., 2010b). However, to our knowledge, studies using the compound specific nitrogen isotopic composition of individual N-containing organic compounds to trace the sources of atmospheric PM are very limited. The lack of studies may be mainly attributed to two factors. First, the marked matrix-related interferences and the relatively low concentrations of individual organic compounds would significantly affect the determination of the $\delta^{15}N$ values for individual N-containing compounds (Ge et al., 2011; Meier-Augenstein, 1999). Second, photochemical decay of most N-containing organic compounds is potentially a very challenging problem. Thus, a high concentration and stability of the compounds in the atmosphere are important factors affecting whether the $\delta^{15}N$ values of specific organic compounds can be used as a fingerprint to identify potential sources.

Amino acids (AAs), one of most ubiquitous compound classes in the atmospheric organic nitrogen fraction, have been found in PM (Samy et al., 2013). In previous AAs composition observations, glycine (Gly) was the most abundant AA species (approximately one-half of the total AAs) in aerosol (Ho et al., 2015; Violaki and Mihalopoulos, 2010). The relatively high proportions and large quantities of Gly in aerosol, provide quantitative guarantees for the compound specific nitrogen isotopic composition analysis.

Stability is an important factor that should be considered when using Gly as a molecular marker. Glycine is usually considered to be a refractory amino acid in the atmosphere (Barbaro et al., 2011; Mandalakis et al., 2011; Scalabrin et al., 2012). Previous studies showed that amino acids existed as zwitterions and had no appreciable absorbance at wavelengths ≥300 nm, so the destruction of amino acids in the atmosphere is not affected by direct photolysis. The destruction of the reactive amino acids in the atmosphere mainly depended upon reaction of their side chains with species such as hydroxyl radical, singlet molecular oxygen, peroxyl radicals, hydrogen peroxide, and excited triplet states (Anastasio and McGregor, 2000, 2001). Due to the absence of a side chain, the activity of Gly in the atmosphere is significantly lower than other amino acids. For instance, the experiments conducted by Anastasio and McGregor (2000) indicated that methionine and tryptophan had half-lives approximately 1–2 h; Histidine and tyrosine had half-lives 13–28 h in midday winter sunlight, which were also significantly destroyed in atmosphere; while glycine is not significantly destroyed during illumination (half-lives>2040 h). They also reported that overall pseudo-first order rate constant for Gly ($<3.4 \times 10\text{-}4 \ h^{-1}$) was much lower than Trp ($9.2 \ h^{-1}$), which had high reactive side chain (Anastasio and McGregor, 2001).

Actually, the origin of the FAAs is still far from being well understood (Matos et al., 2016). It is generally accepted that free AAs (FAAs) in the aerosols could primarily derived from biogenic natural sources (e.g., plants, pollen, soil, terrestrial dust, fungi and spores) (Huffman et al., 2013; Joung and Buie, 2015; Scalabrin et al., 2012; Scheller, 2001). Other likely sources include biomass burning (Barbaro et al., 2019; Mace et al., 2003) and cooking emissions (Abe et al., 2015) etc. In addition, fossil fuel combustion is also suggested to be a source of FAAs in aerosol (Ren et al., 2018; Song et al., 2017). The organic fraction (humic acid and undecomposed plant material) is an important precursor of fossil fuel. This fraction contains a large quantity of proteinaceous materials,

but experiences a lengthy diagenesis during the formation of coal (Casagrande et al., 1980). Unfortunately, there are limited measurements of FAAs released from fossil fuel combustion. It is believed that Gly is refractory and its structure is not destroyed in the photochemical processes within aerosols (Dauwe et al., 1999; Liu et al., 2017). These imply that isotope effect associated with the degradation of proteinaceous material in aerosol may be relatively small. The $\delta^{15}N$ values of free Gly released from natural sources may reflect its values in primary emission sources. Up to now, the $\delta^{15}N_{F\text{-}Gly}$ values from the different primary emission sources are still ambiguous. It is unclear whether Gly directly released from different sources has different nitrogen isotopic compositions. Thus, in this paper we investigated the nitrogen isotopes of free Gly in potentially primary emission sources (plant, soil, biomass burning, fossil fuel combustion, kitchen fumes). Furthermore, the free Gly levels and $\delta^{15}N_{F\text{-}Gly}$ values of total suspended particles (TSP) collected in the Yudu forest are analyzed. Then, the $\delta^{15}N_{F\text{-}Gly}$ values in Yudu forest aerosol are compared with the data of the fire point and the K^+ levels, which is used to indicate biomass burning. The following questions are discussed: (1) Are the isotopic differences of the $\delta^{15}N_{F\text{-}Gly}$ values large enough to distinguish the different aerosol sources? (2) Could the $\delta^{15}N_{F\text{-}Gly}$ values in the aerosol be used to trace biomass burning? To our knowledge, this is the first study presents information about $\delta^{15}N_{F\text{-}Gly}$ values in different aerosol sources.

2. Materials and methods

2.1. Sample collection

2.1.1. TSP sample collection

Forest TSP samples (n = 29) were collected at a forest site (25°54′36″N, 115°37′44″N) in Yudu county, Jiangxi province, China from January 1 to February 27, 2018. The sampling site was in a forested area, which was away from cities and not polluted by anthropogenic N sources. For Gly measurements, sampling was conducted on the rooftop of a six-story building (~18 m agl above ground level) using a high-volume air sampler that pumped ambient air at 1050L min^{-1} through 25 × 20 cm quartz fiber filters. Before sampling, quartz fiber filters were heated at 450 °C for 10 h to remove any organics. For forest aerosol sampling, the collection time was 48 h. Filters were stored at −20 °C prior to analysis.

2.1.2. Plant collection

During July 2017, Masson pine (*Pinus massoniana* (Lamb.)) and moss samples (*Haplocladium microphyllum* (Hedw.)) were collected in Nanchang city. The Masson pine tree chosen for sampling was approximately 10 years old and 4 m in height. Only green, healthy samples were collected. Eligible sampling sites were chosen according to our previous studies (Xiao et al., 2010a; Xu and Xiao, 2017).

2.1.3. Soil collection

Paddy soil samples were collected from the topmost 10 cm layer of the soil in Nanchang city (115.1°E, 28.2°N), where rice cultivation is maintained. After sampling, any roots and litter were removed immediately. Road soil was collected from the surface of a tunnel in Guiyang city (106.7°E, 26.7°N).

2.1.4. Biomass burning emissions

Biomass fuels, extensively used in rural China for cooking and heating, emit large quantities of air pollutants (Li et al., 2014; Liu et al., 2016). Tao et al. (2018) found that wood (mainly pinewood) and crop residues (mainly straw) are the major contributors toward the heating energy in China, and accounts for 33% and 14% respectively. Based on the results, pine-wood and straw were selected as sources of biomass burning and the $\delta^{15}N_{F\text{-}Gly}$ in the aerosol particles from pine wood and straw burning were analyzed in this study.

High-volume air samplers were deployed during August 2017 to

sample free Gly emitted from biomass burning. In laboratory tests, emissions from the stove were collected using a large iron exhaust hood and then sampled into the high-volume air sampler for aerosol source sample collection. Aerosols from biomass burning were sampled at 1 m above the fire level. For the pine biomass burning emissions, leaves and smaller branches were burned in honeycomb briquette heating stove; straw was burned in cooking stoves. Burns typically lasted 5–15 min.

2.1.5. Kitchen fumes

Free Gly emitted from kitchen emissions were sampled in August 2017 during supper time. Samples were collected from a kitchen exhaust vent at a barbecue restaurant, where fried meats and fried vegetables were continuously cooked. An electric furnace was used in the kitchen for cooking. Collection typically lasted from 1 to 3 h.

2.1.6. Coal combustion emissions

A high-volume air sampler was deployed downwind from the honeycomb briquette heating stove in August 2017 to collect free Gly emitted from coal combustion. A single collection of 1–2 h was performed during the coal combustion process.

2.1.7. Vehicle emissions

In August 2017, high-volume air samplers, attached to the exhaust pipes of idling vehicles, collected free Gly samples emitted from an assortment of diesel and commercial vehicles, engines, and fuel types. Of the surveyed vehicles, BYD L3, Golf and Audi A3 used gasoline; BYD L3 and Golf used 92# gasoline and, Audi A3 used 95#gasoline. Changzhou R180 operated on diesel. All vehicles were idling during the sampling period. The sample collection time was 3 h.

2.2. AA concentration and isotopic analysis

The dissolved FAAs were extracted by Milli-Q water and analyzed using the method proposed by Mandalakis et al. (2011). 2-Aminobutyric acid (AABA) was added as an internal standard. Purified AAs were analyzed as AA–tert-butyl dimethylsilyl (tBDMS) derivatives (Zhu et al., 2018).

The free Gly concentrations and $\delta^{15}N_{F\text{-Gly}}$ were analyzed using a gas chromatograph-mass spectrometer (GC-MS)/isotope ratio MS (IRMS). The GC-MS/IRMS instrument was composed of a Thermo Trace GC (Thermo Scientific, Bremen, Germany) whose output was split, with approximately 10% directed into a Thermo ISQ QD single quadrupole MS that provided structural and concentration information for each eluting peak. The remaining ~90% passed through a GC-isolink, where eluting AAs were oxidized and reduced to form N_2. These gases were finally directed into a Thermo Delta V IRMS (Thermo Scientific, Bremen, Germany) for $\delta^{15}N$ measurement. The GC column and conditions employed during GC-MS/IRMS analysis are described earlier (Zhu et al., 2018).

The single quadrupole MS was operated in electron impact ionization (70 eV electron energy) and full scan mode. The temperatures of the transfer line and ion source were kept constant at 250 °C and 200 °C, respectively. Further detail on the GC-MS results, including quality assurance and control (recoveries, linearity, detection limits, quantitation limits, and corresponding effective limits in the aerosol samples of AAs), are available in the Supporting Information (Table S1).

To evaluate the precision of the method and to calibrate the instrument, a wide-range (from −26.63‰ to +40.83‰) isotopic reference materials of Gly (Schimmelmann et al., 2016), which are commercially available from Indiana University (http://php.indiana.edu/~aschimme/hc.html) and two high purity standards (purities >99%) were employed (Table S2). A linearly correlation between the $\delta^{15}N$ values of underivatized Gly and those of the Gly-tBDMS derivatives ($R^2 = 0.997$, $P < 0.001$) were obtained (Fig. S1). Gly standards were also analyzed after every three samples collected during the GC-MS/IRMS analytical sessions. Moreover, the internal standard (AABA) with a known $\delta^{15}N$ value added in each sample was checked to confirm the reproducibility of the isotope measurements.

The amount required for $\delta^{15}N_{F\text{-Gly}}$ analysis using the GC-MS/IRMS instrument is an important parameter. Gly standards amount of 0.2–3 nmol was injected; the accuracy and precision of the $\delta^{15}N$ values are shown in Table S3. The precision of the $\delta^{15}N$ measurements (n = 3) for the derivatized mixture of AA standards ranged from 0.2‰ to 2.2‰. The difference between the Gly $\delta^{15}N$ values measured using EA/IRMS and by GC-MS/IRMS after empirical correction ranged from 0.2‰ to 0.6‰ (Table S3). Aerosol samples had to be concentrated to obtain adequate amount of Gly for the $\delta^{15}N$ measurements. Each reported value is a mean of at least three $\delta^{15}N$ determinations.

2.3. Other chemical components analysis

Water-soluble ions (Na^+, NH_4^+, K^+, Mg^{2+}, Ca^{2+}, F^-, Cl^-, NO_3^-, formic acid, Oxalic acid and SO_4^{2-}) were measured by ion chromatography (DIONEX AQUION, Thermo Scientific, Bremen, Germany).

2.4. Statistical analysis

Statistical analysis was conducted by using SPSS 16.0. Significant differences in the FAA contents among the various emission sources were tested using the one-way analysis of variance (ANOVA) procedure, and compared using the Tukey-HSD test; differences were considered significant at $P < 0.05$. Pearson's correlations were conducted to examine the relationship between the free Gly concentration and non-sea-salt potassium ion (nss-K^+) levels; the logarithmic regression was analyzed to evaluate changes in $\delta^{15}N_{F\text{-Gly}}$ as a function of nss-K^+. Graphs were mainly generated using OriginPro 2017. The results of the two-day air mass backward trajectory analyses at 100 m height (above sea level) and the fire spots were calculated every 6 h using TrajStat software (Wang et al., 2009).

3. Results

3.1. $\delta^{15}N_{F\text{-Gly}}$ values of major emission sources

Currently, it is difficult to use AAs as molecular tracers to track the sources of aerosol PM because of the lack of AA $\delta^{15}N$ information from emission sources. In this study, the potential $\delta^{15}N_{F\text{-Gly}}$ emission sources including plants, soil, biomass burning, coal combustion, kitchen fumes, and vehicle emissions are summarized in Table 1. The $\delta^{15}N_{F\text{-Gly}}$ values of the major emission sources varied widely from −16.6‰ to +22.6‰. The range of $\delta^{15}N_{F\text{-Gly}}$ released by major sources was quite different. The $\delta^{15}N_{F\text{-Gly}}$ variation ranges for major emission sources are presented in the following sections.

3.1.1. Natural sources

Plant and soil samples, important parts of natural sources, were analyzed in this study. For plants tissues sampled in this study, free Gly exhibited negative $\delta^{15}N$ signatures. The $\delta^{15}N_{F\text{-Gly}}$ values in mosses and pine needles were on average −14.3 ± 2.7‰ and −11.7 ± 1.8‰ respectively. In contrast, paddy soil (+1.7 ± 0.8‰) and tunnel soil (+7.5 ± 1.9‰) had more positive $\delta^{15}N_{F\text{-Gly}}$ values than those in plants tissues (Table 1). Moreover, the differences in the $\delta^{15}N_{F\text{-Gly}}$ values were significant between the plants (−13.6 ± 2.5‰) and soil (+4.6 ± 4.0‰) (one-way ANOVA, $p < 0.05$).

3.1.2. Kitchen fumes

Free Gly collected from kitchen fumes exhibited relative positive $\delta^{15}N$ values with a mean of +6.0 ± 1.5‰ (range: +4.5‰ to +7.8‰), which were significantly higher values than those of plants (−13.6 ± 2.5‰) but significantly lower than those of biomass burning (one-way ANOVA, $p < 0.05$). Unfortunately, the ranges of the $\delta^{15}N_{F\text{-Gly}}$ values in kitchen fumes and soils were overlapped (Table 1).

ARTICLE IN PRESS

R.-g. Zhu et al.   Atmospheric Environment xxx (xxxx) xxx

Table 1
Nitrogen isotopic composition of free Gly from plant, soil, coal combustion, vehicle exhaust and kitchen fumes from this study.

Source	Sampling method	$\delta^{15}N_{F\text{-}Gly}$ (‰)
Natural sources		
Plant		
Mosses	*Haplocladium microphyllum* tissues; n = 19	−14.3 ± 2.7
Pine	*Pinus massoniana* (Lamb.) needles; n = 6	−11.7 ± 1.8
Mean		*−13.6 ± 2.5*
Soil		
Paddy soil	clay; 0–10 cm depths; maintained in rice cultivation; n = 4	+1.7 ± 0.8
Tunnel soil	road soil from Huoyanshan tunnel in Guiyang city; n = 6	+7.5 ± 1.9
Mean		*+4.6 ± 4.0*
Kitchen fumes		
Kitchen exhaust	from kitchen exhaust vent, electric furnace	+4.5
Kitchen exhaust	from kitchen exhaust vent, electric furnace	+5.1
Kitchen exhaust	from kitchen exhaust vent, electric furnace	+6.5
Kitchen exhaust	from kitchen exhaust vent, electric furnace	+7.8
Mean		*+6.0 ± 1.5*
Biomass burning		
Pine	Pine wood; honeycomb briquet heating stove	+17.7
Pine	Pine wood; honeycomb briquet heating stove	+16.9
Straw	Straw; wood-fired cook stove	+22.7
Straw	Straw; wood-fired cook stove	+27.3
Straw	Straw; wood-fired cook stove	+27.2
Mean		*+22.4 ± 5.0*
Fossil fuel		
Coal combustion		
Bituminous	bituminous coal; honeycomb briquet heating stove	NA
Bituminous	bituminous coal; honeycomb briquet heating stove	NA
Bituminous	bituminous coal; honeycomb briquet heating stove	NA
Honeycomb briquet	Anthracite added yellow clay soil; honeycomb briquet heating stove	NA
Honeycomb briquet	Anthracite added yellow clay soil; honeycomb briquet heating stove	+22.6
Vehicle exhaust		
Diesel exhaust	diesel engine; rpm 2600r/min	NA
Diesel exhaust	diesel engine; rpm 2600r/min	NA
BYD exhaust	BYD L3; gasoline engine; 92#;;rpm 1000r/min	NA
BYD exhaust	BYD L3; gasoline engine; 92#;;rpm 1000r/min	NA
Golf exhaust	Golf 1.7; gasoline engine; 92#;;rpm 1000r/min	NA
Golf exhaust	Golf 1.7; gasoline engine; 92#;;rpm 1000r/min	NA
Audi exhaust	Audi A3; gasoline engine; 95#;;rpm 1000r/min	NA
Audi exhaust	Audi A3; gasoline engine; 95#;;rpm 1000r/min	NA

3.1.3. Biomass burning emissions

In general, free Gly emitted from biomass burning demonstrated very positive $\delta^{15}N$ values. These are the first measurements of the $\delta^{15}N$ values of free Gly in aerosol particles from biomass burning. The $\delta^{15}N_{F\text{-}Gly}$ values from pine wood burning were +17.7‰ and +16.9‰ (n = 2). The $\delta^{15}N_{F\text{-}Gly}$ values from straw burning ranged from +22.7‰ to +27.3‰ with a mean of +25.7 ± 2.6‰ (n = 3) (Table 1). The nitrogen isotope values for free Gly in the aerosol particles collected during biomass burning (+22.4 ± 5.0‰) were significantly positive than those of two types of plants collected in this study (−13.6 ± 2.5‰) (one-way ANOVA, p < 0.05), with a difference of 36‰ between the average values. This indicates that free Gly in particulates released by biomass burning was preferentially enriched in ^{15}N.

3.1.4. Fossil fuel

3.1.4.1. Coal combustion. Bituminite coal, is usually burned in industrial boilers, while honeycomb briquette, made from bituminite and clay, is burned for residential coal combustion in China (Zhang et al., 2008). Aerosol samples from bituminite combustion (n = 3) and honeycomb briquette combustion (n = 2) were collected in this study. Free Gly concentrations from bituminous combustion were below the limit of detection (0.1 pmol m^{-3}) for the analytical procedure, suggesting that bituminous combustion may not be the source of free Gly in aerosol.

Interestingly, free Gly was detected in aerosol particles released by combustion of honeycomb briquette. This result was expected because honeycomb briquettes are made from clay; free Gly released during honeycomb briquette combustion may be derived from clay decomposition during the combustion procedure. Furthermore, the $\delta^{15}N_{F\text{-}Gly}$ value produced by the burns of honeycomb briquette (+22.6‰) was also ^{15}N-enriched by 18‰ relative to the average $\delta^{15}N_{F\text{-}Gly}$ value in unburned soil (+4.6 ± 4.0‰), suggesting that the free Gly released by honeycomb briquette combustion was also significantly enriched in ^{15}N.

3.1.4.2. Vehicle emissions. To assess whether vehicle emissions are the primary source of free Gly in aerosols, aerosol sample were collected outside of the exhaust pipe of vehicles using different engines (e.g., diesel engines and gasoline engines) and different fuel types (e.g., diesel, 92# gasoline and 95# gasoline) (Table 1). However, no free Gly was measured in the captured particulates from all vehicle emission. Thus, free Gly emitted from vehicle exhaust was, if present, below 0.1 pmol m^{-3}, we conclude that vehicle emissions might not be a major source of free Gly in atmospheric PM.

3.2. Free Gly in aerosol

Fig. 2 shows the temporal variations in the TSP $\delta^{15}N_{F\text{-}Gly}$ values collected in the Yudu forest and in active fire spots located in two-day air mass backward trajectories. The isotopic composition of free Gly in Yudu forest aerosols ranged from −4.6‰ to +21.8‰, with a mean of +11.4 ± 6.0‰ (n = 29). In this study, the fire spots surrounding Yudu forest were derived from NASA Earth Observatory's Active Fire Data (https://earthdata.nasa.gov/earth-observation-data/near-real-time/firms/active-fire-data#tab-content-6). The $\delta^{15}N_{F\text{-}Gly}$ values and fire points exhibited the same temporal pattern in the Yudu forest. The isotopic composition of free Gly in forest aerosols with fewer fire points ranged from −4.6‰ to +3.3‰ (Jan 5–6 and Jan 25–30), which was close to the values of free Gly from natural sources (e.g., plants, soil, microbes, and animal debris). The isotopic composition of Gly in forest aerosols with more fire points demonstrated more positive $\delta^{15}N$ signatures and, ranged from +10.1‰ to +21.8‰ (Jan 1–4, Jan 9–16, Feb 2–7, Feb 10–17 and Feb 18–27), which implies an influence from biomass burning (Fig. 2). In brief, more positive $\delta^{15}N$ signatures of free Gly were observed during the periods influenced by a higher contribution from biomass burning.

Moreover, there was positive correlation between the free Gly and nss-K$^+$ levels for TSP samples in the Yudu forest (y = 144.30 + 351.73x, R = 0.576, P < 0.05) (Fig. 3B), not including data from Feb 14 to 17. Those four days are the Chinese Lunar New Year. Setting fireworks is one of the traditional customs of the Spring Festival. Potassium is usually one of the components of fireworks and, an abnormally high potassium level was observed during this period. Additionally, there was a good correlation between the $\delta^{15}N_{F\text{-}Gly}$ value and the logarithm of the nss-K$^+$ concentration (y = 14.23 + 3.64x, R = 0.608, P < 0.05) (Fig. 3A).

ARTICLE IN PRESS

R.-g. Zhu et al.   Atmospheric Environment xxx (xxxx) xxx

4. Discussion

Previously, the concentrations and molecular compositions of FAA have been used to trace the source and atmospheric processes of AAs in aerosol (Barbaro et al., 2015; Ren et al., 2018; Scheller, 2001; Wedyan and Preston, 2008), but the $\delta^{15}N$ values of free Gly in aerosol have not yet been determined. It is unclear whether the nitrogen isotope values of free Gly in aerosol would probably be used to trace biomass burning.

4.1. Nitrogen isotope fractionation of Gly associated with biomass burning

In previous studies, factor analysis and factor-analysis-based approaches such as positive matrix factorization (PMF) offer the possibility that biomass burning is a potential source of FAAs in aerosol (Barbaro et al., 2019; Mace et al., 2003; Song et al., 2017; Violaki and Mihalopoulos, 2010). Nitrogen isotopes has been demonstrated to be an effective tools to investigate the sources of atmospheric N deposition. However, direct laboratory and field measurements of the $\delta^{15}N_{F-Gly}$ values in biomass burning aerosols are very limited. In this study, the $\delta^{15}N_{F-Gly}$ values from natural source profiles were pooled from multiple samples collected from literature data, where possible. Compared with the $\delta^{15}N_{Gly}$ values from natural source profiles, we found the $\delta^{15}N_{F-Gly}$ values in the aerosol particles from biomass burning (range: +16.9‰ to +27.3‰) were more positive than those observed from natural sources, such as plants (range: −23.5‰ to +5.0‰), soil (range: +1.2‰ to +9.4‰), animal debris (range: +6.1‰ to +7.6‰), and microbes (range: +5.3‰ to +5.7‰) (Fig. 1). Similarly, a marked positive $\delta^{15}N$ value was observed for combined Gly (+10.7‰) in fossil soil affected by burning turf dung and seaweed (Simpson et al., 1999).

The $\delta^{15}N$ values of Gly in atmospheric particles are associated with the hydrolysis of higher molecular weights proteinaceous material (HMW) or peptides and whether the FAAs produced are further degraded (Fig. 4, green shadow). Photochemical hydrolysis (oxidative attack of •OH) and enzymatic hydrolysis of HMW or peptides are proved to be the main formation processes of FAAs in aerosols (Milne and Zika, 1993; Mopper and Zika, 1987; Song et al., 2017). In photochemical hydrolysis process, oxidants preferentially attack the polypeptide backbone of peptides due to low steric hindrance of Gly (Liu et al.,

2017). As a result, the higher yield of free Gly than other amino acid was observed in photochemical hydrolysis of proteinaceous material. Similarly, Gly tend to be preserved under microbial-related enzymatic cleavage processes because Gly is mainly in the cell wall whereas those FAAs, which concentrated in cell plasma, are easy to be degraded and thus depleted (Dauwe et al., 1999; Yan et al., 2015). Furthermore, released Gly is difficult to be degraded in natural processes due to the absence of side chain (Fig. 4, green shadow). These suggest that it is difficult for the structure of free Gly to be destroyed by photochemical and microbial-related enzymatic processes in the atmosphere. Therefore, free Gly produced by natural processes may have a $\delta^{15}N$ value very similar to that of primary natural sources.

In biomass burning events, however, a large portion of free Gly was degraded and amino-N loss through the C–N cleavage of the amino-N of Gly was observed (Anca-Couce et al., 2018; Zhou et al., 2017). And some ^{15}N-depleted volatile nitrogen such as gases NH_3 is preferentially released from C–N cleavage of the amino-N of Gly during biomass burning, leaving residual free Gly ^{15}N-enriched, then those ^{15}N-enriched free Gly entered the atmosphere and kept stable in aerosols (Fig. 4, red shadow). Kundu et al. (2010) suggested that particles produced from combustion are composed of a wide variety of volatile nitrogen compounds, which come from the fuel nitrogen. However, the formation mechanism and distribution for volatile nitrogen compounds during different biomass burning stages differ greatly. In the first combustion phase (devolatilization), fuel-N (mainly protein-N) is converted to volatile nitrogen such as gases NH_3 by splitting amine N-tar (primary tars) at temperatures lower than 500 °C. At higher temperatures (>500 °C), some volatile N was oxidized to NOx (Anca-Couce et al., 2018). During low rank fuels (e.g., wood and straw) burning, volatile-N compounds were found to be mainly released as NH_3 from the amines-N of fuel (Vermeulen et al., 2012). Furthermore, temperature is the key factor affecting the mechanism and amount of NH_3 released. Zhou et al. (2017) suggested three stages of biomass pyrolysis. In the first stage (<300 °C), the decomposition of labile protein mainly occurred, producing a small amount of NH_3. In the second stage (300–600 °C), the protein-N started to split into small molecular amine compounds, then went through a deamination process and produced a large quantity of NH_3. In the third stage (600–900 °C), the amine compounds were converted into a large amount of HCN. That is, the reaction of the amino-N loss through the
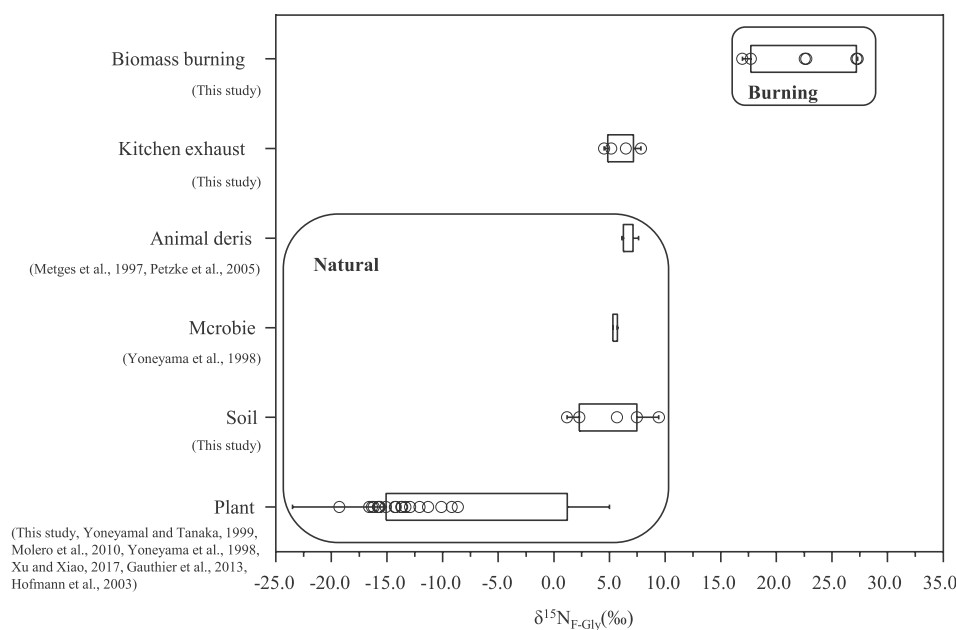

Fig. 1. The range of δ15N for free Gly from major emission sources. Open circles represent the isotopic composition data of free Gly in this study. The box encloses 50% of the data reported in previous studies and in this study, the whiskers is the range of the data.
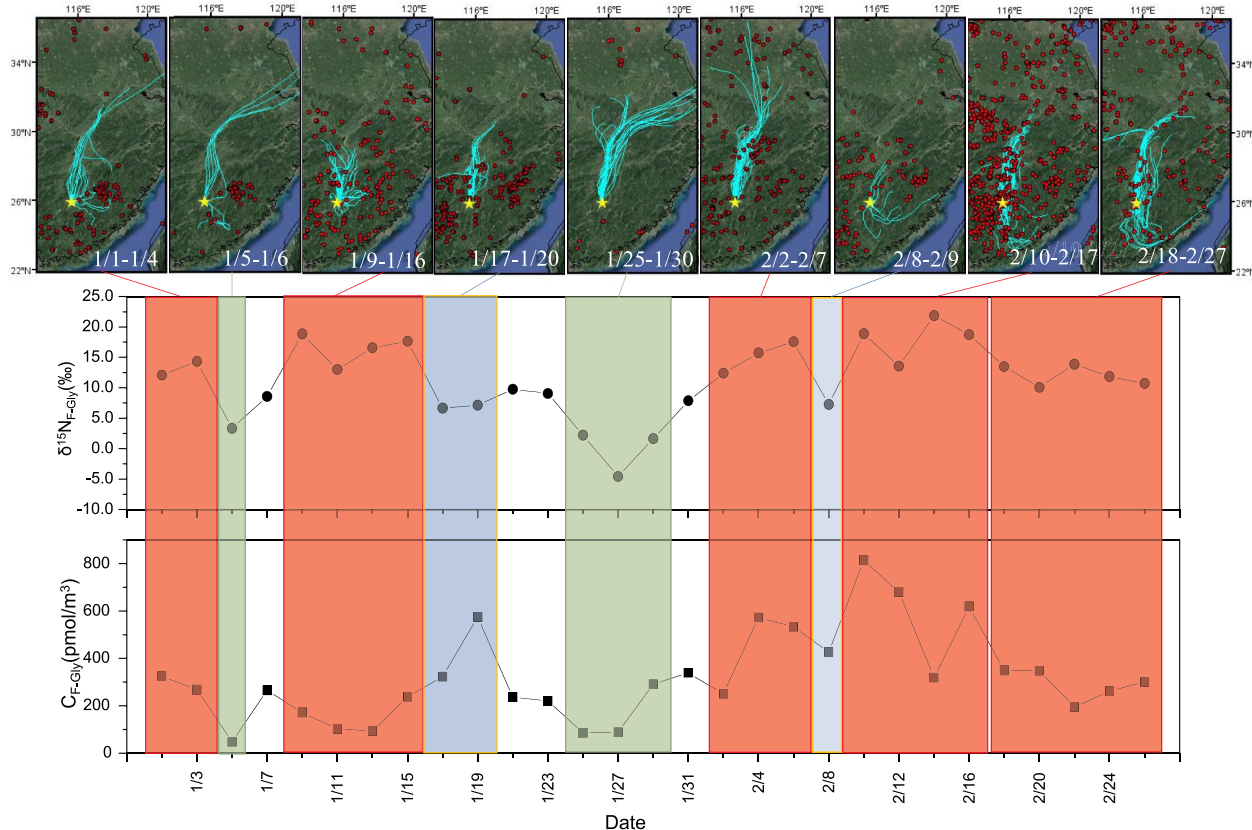
ARTICLE IN PRESS

R.-g. Zhu et al.   Atmospheric Environment xxx (xxxx) xxx

Fig. 2. Temporal trends of δ15NF-Gly values in TSP collected in Yudu forest during the sampling period. Two-day air mass back trajectories arriving at 100 m (above sea level) over Yudu forest. Yellow star represent the sampling site. Fire spot data that were arrived from NASA are present in red. (For interpretation of the references to colour in this figure legend, the reader is referred to the Web version of this article.)
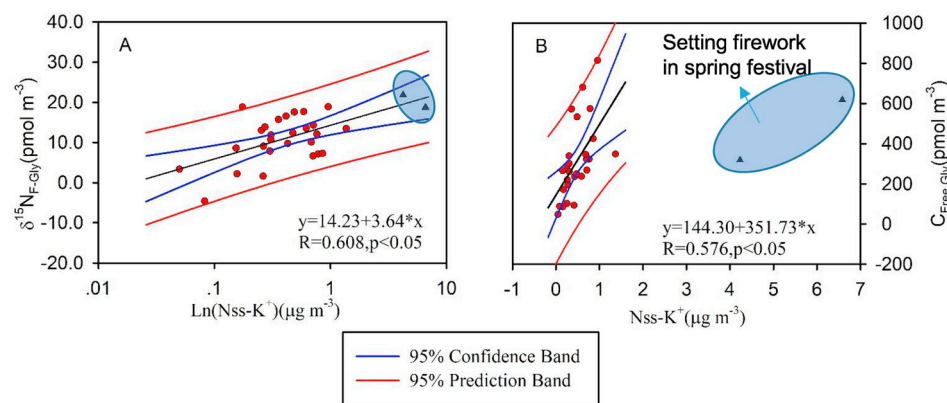

Fig. 3. Relationship between δ15NF-Gly values (‰) (A), the concentration of free Gly (pmol m-3) (B) and non-sea-salt potassium (nss-K+) (µg m-3) in TSP collected from Yudu forest. Triangles represents the samples significantly affected by fireworks during spring festival, and these samples were excluded from regression analysis. The black line denotes a linear regression fit, the blue line denotes 95% confidence band, the red line denotes 95% prediction band. [nss-K+] = [K+] − [Na+] × 0.037 (Ren et al., 2018). (For interpretation of the references to colour in this figure legend, the reader is referred to the Web version of this article.)

C–N cleavage of the amino-N of Gly was shown to occur in the biomass burning procedure, and the amount of NH_3 released was significantly elevated when the temperature rose above 300–500 °C, which is significantly different to the atmospheric conditions. That's why a large portion of free Gly in degraded in biomass burning whereas this reaction was not occurred after it enters into the atmosphere.

Although isotope fractionation associated with C–N cleavage of the amino-N atom of Gly occurred in biomass burning has never been measured; the isotope fractionation associated with NH_3 loss from the amino-N atom of glutamic acid is 14‰ against ^{15}N (Tcherkez, 2011). O'Leary et al. (1974) found that such a sizable value coincided with the isotope fractionation of 25‰ associated with non-enzymatic, rate-limiting C–N breaking in organic reactions. This finding has led to the

suggestion that biomass burning derived NH_3 may have a more depleted ^{15}N value than that in biomass fuel and a marked positive $\delta^{15}N$ value may preserved in remaining Gly. Correspondingly, Turekian et al. (1998) attributed bulk $\delta^{15}N$ enrichment in biomass burning aerosol particles to the preferential loss of ^{14}N gaseous nitrogen from the organic pool. Turekian et al. also proposed that the lost nitrogen came from deamination of AAs.

Whilst the $\delta^{15}N$ values of free Gly released from different biomass types showed some variability, the nitrogen isotopic fractionation associated with NH_3 loss from the amino-N atom of Gly during biomass burning (temperature above 300–500 °C) leads to a large difference in the $\delta^{15}N_{F-Gly}$ values between biomass burning and natural sources (Fig. 4). Therefore, the possibility of using the nitrogen isotope of free

ARTICLE IN PRESS

R.-g. Zhu et al.   Atmospheric Environment xxx (xxxx) xxx
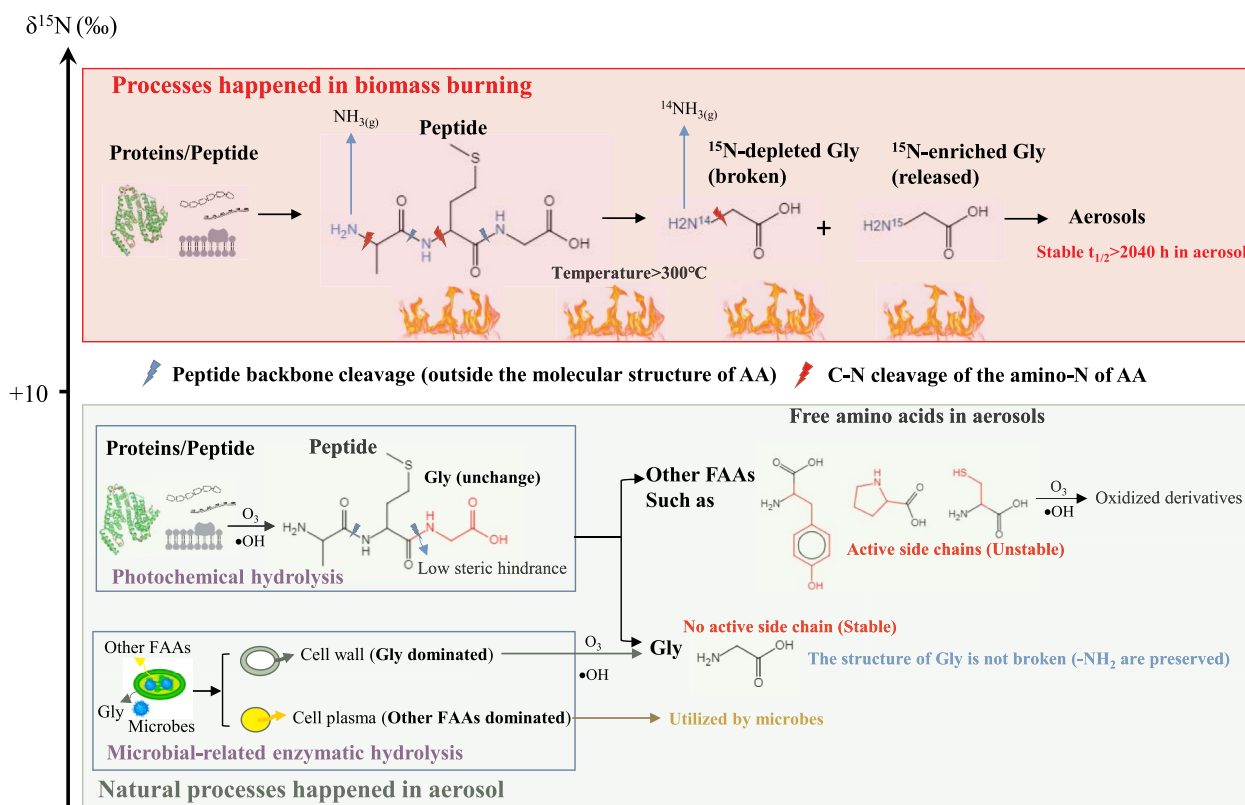

Fig. 4. The specific processes of free-glycine in aerosols and biomass burning events.

Gly to identify the contribution of biomass burning in atmospheric PM could be based on the significantly different δ^{15}N values between biomass burning and natural sources.

4.2. Nitrogen isotope fractionation of Gly associated with cooking

Our results demonstrates that cooking does not introduce significant nitrogen isotopic modifications in free Gly, which is in agreement with previous results. Deniro et al. (1985) reported that boiling or roasting did not change the δ^{15}N values of bone by more than 1‰. Fernandes et al. (2014) investigated the influence of cooking on the nitrogen isotope values of raw fish flesh using three cooking methods (boiled, roasted, and steamed). Their results also indicated that nitrogen isotopic changes in the bulk flesh and bone collagen of fish during cooking were smaller than 1‰. They attributed this result to preferential losses of volatile nitrogen (e.g., NH_3) that were not large enough to meaningfully modify isotopic values.

However, under more extreme heating (temperature higher than 295 °C), large shifted bulk δ^{15}N values of bone 4‰ were observed (Deniro and Hastorf, 1985). As discussed above, temperatures was the key factor controlling the amount of NH_3 released from amino-N, and the amount of released NH_3 is small when the temperature is below 300 °C. Thus, we can infer that modifications to $\delta^{15}N_{F\text{-}Gly}$ caused by cooking were smaller than that of biomass burning, probably because of the losses of the volatile-N compounds (NH_3) were not enough to modify the $\delta^{15}N_{F\text{-}Gly}$ values.

4.3. Free Gly released from fossil fuel combustion

Fossil fuel has long been considered an important source of anthropogenic pollutant emissions (Bond et al., 2004; EPA, 2009). Although undecomposed plant material is an important precursors of fossil fuel, free Gly in aerosol samples from bituminous coal combustion and all vehicle exhaust, including diesel and gasoline engines, were below

effective limit in the aerosol samples (EMDL) (0.1 pmol m^{-3}) in this study. Previous studies have found that in the stage of coalification, the original organic nitrogen is mainly transformed to pyridine, pyrrolic, quaternary nitrogen and nitrogen oxides (Kelemen et al., 1994). In a study carried out by Zhang et al. (2008), approximately 200 organic compounds were quantified from anthracite, bituminite, and brown coal combustion; however, no AAs have been detected in their study. Similarly, no AAs have been detected in particulates of vehicle emissions until now (Ge et al., 2011; Rui et al., 2009). Thus, we could infer that bituminous combustion and vehicle emissions may not be the sources of FAAs in the aerosol.

However, it was unexpectedly discovered that free Gly is emitted from honeycomb briquette combustion, which may be because biomass materials (clay) are usually added during the production of residential coal. A noticeably ^{15}N-enriched signature of free Gly formed by the combustion of honeycomb briquette (+22.6‰) was observed in this study, which may be attributed to the added biomass (clay) combustion and the fractionation associated with the deamination of Gly during the combustion process, as discussed above. Solid fuels (e.g., honeycomb briquette) are extensively used in most rural and suburban areas in China for domestic heating and cooking purposes, especially during the winter (Duan et al., 2014; Zhang et al., 2017); residential coal combustion might be a potential source of aerosol AAs in China, particularly in rural and suburban areas. Therefore, a better understanding of the potential emissions contributions from residential coal would help to accurately estimate the impact of biomass burning on air quality in China.

4.4. Using δ^{15}N values of free Gly to identify biomass burning

A potential correlation between the free Gly concentrations and biomass burning aerosols has been suggested in past studies. For instance, a significant correlation is observed between Gly and elemental carbon (EC) in Eastern Mediterranean aerosol (Violaki and

Mihalopoulos, 2010). Samy et al. (2013) observed the significant positive correlations ($p < 0.002$) between free Gly and biomass burning related N-heterocyclic compounds. In our study, a high correlation between free Gly and nss-K$^+$ ($R^2 = 0.68$, $p < 0.01$) was also observed (Fig. 3B). Because nss-K$^+$ is a tracer of biomass burning activities (Kunwar and Kawamura, 2014), the contribution of the combustion processes to the Gly levels in aerosol was confirmed. This contribution may be attributed to free Gly being directly emitted from biomass burning (Chan et al., 2005). Additionally, unlike nss-K$^+$(Wang et al., 2007), the concentration of the free Gly in aerosol was not influenced by setting off fireworks (Fig. 3B).

Furthurmore, as we discussed above, biomass burning contributes markly enriched $\delta^{15}N$ values to atmospheric free Gly relative to existing data for natural sources. Thus, we inferred that $\delta^{15}N_{F\text{-Gly}}$ might be used in tracking biomass burning. These are the first measurements of $\delta^{15}N_{F\text{-Gly}}$ values in aerosol samples, as such, there are no other data to compare them with directly. To test the possibility of using $\delta^{15}N_{F\text{-Gly}}$ in aerosol to identify biomass burning, the $\delta^{15}N_{F\text{-Gly}}$ values collected at the Yudu forest were compared with fires spots located in two-day air mass backward trajectories (Fig. 2). The influence of the expected change in the contribution of biomass burning on the nitrogen isotopic composition of free Gly in aerosol depends on the emission fluxes and N isotopic composition from major free Gly sources (e.g., natural sources and biomass burning). This study provides important constraints on the nitrogen isotopic composition of major free Gly emission sources (Fig. 1). Increased contributions from biomass burning sources will result in more positive aerosol $\delta^{15}N_{F\text{-Gly}}$ values. This was further supported by the nitrogen isotopic composition of free Gly in aerosol, collected during period that was significantly influenced by biomass burning (more fire spots) in Yudu forest ($+10.1‰ \sim +21.8‰$), were more positive and close to the range of biomass burning ($+16.9‰ \sim +27.3‰$). While the samples collected during the period that was less influenced by biomass burning (fewer fire spots) ($-4.6‰ \sim +3.3‰$) were more depleted and fall in the range of plant ($-23.5‰ \sim +4.6‰$) and soil sources ($+1.2‰ \sim +9.4‰$) (Fig. 2). Moreover, a link between the $\delta^{15}N_{F\text{-Gly}}$ values and nss-K$^+$ was found in this study. Therefore, we suggested that the aerosol $\delta^{15}N_{F\text{-Gly}}$ values may be useful for identifying biomass burning.

The potential limitations in this study include that the degree of kinetic fractionation varied with the different biomass types, and the types of fire (stack fires, chamber fires) were not evaluated. To further reduce the uncertainty in using $\delta^{15}N_{F\text{-Gly}}$ values to indicate potential sources, additional experiments are required to more comprehensively characterize the fractionation process under different biomass types and burning conditions.

5. Conclusions

The present study is the first to investigate the nitrogen isotope compositions of potential emission sources of free Gly in aerosol including plants, soil, biomass burning, coal combustion, kitchen fumes and vehicle emissions. Additionally, temporal variations in the $\delta^{15}N_{F\text{-Gly}}$ values in TSP collected in Yudu forest were analyzed. The main findings are listed below:

i. The $\delta^{15}N$ values of free Gly emitted from biomass burning are more positive than those from natural sources, such as plants, soil, animal debris and microbes.

ii. Bituminous combustion and vehicle emissions may not be the source of free Gly in the aerosol. Honeycomb briquette combustion may be a potential source of aerosol AAs in China, particularly in rural and suburban areas. This may be attributed to added biomass (clay) in honeycomb briquette.

iii The results reported here are the first to suggest that the $\delta^{15}N$ values of free Gly might be used in tracing biomass burning. This conclusion is supported by the $\delta^{15}N_{F\text{-Gly}}$ values and fire points showed the same

temporal pattern in Yudu forest. Moreover, a link between the $\delta^{15}N_{F\text{-Gly}}$ values and nss-K$^+$ was found.

Author contributions section

Ren-guo Zhu and Hua-Yun Xiao conceived and designed the experiments; Hongwei Xiao, Zhe Lv and Hao Xiao collected the aerosol samples; Ren-guo Zhu, Zhongyi Zhang and Nengjian Zheng performed the experiments; Ren-guo Zhu analyzed the data; Hua-Yun Xiao and Hongwei Xiao contributed reagents and analytical tools. Ren-guo Zhu wrote the paper. All authors reviewed and approved the final version of manuscript.

Declaration of competing interest

The authors declare that they have no known competing financial interests or personal relationships that could have appeared to influence the work reported in this paper.

Appendix A. Supplementary data

Supplementary data to this article can be found online at https://doi.org/10.1016/j.atmosenv.2019.117179.

References

Abe, R.Y., Akutsu, Y., Kagemoto, H., 2015. Protein amino acids as markers for biological sources in urban aerosols. Environ. Chem. Lett. 14, 1–7.

Anastasio, C., McGregor, K.G., 2000. Photodestruction of dissolved organic nitrogen species in fog waters. Aerosol Sci. Technol. 32, 106–119.

Anca-Couce, A., Sommersacher, P., Evic, N., Mehrabian, R., Scharler, R., 2018. Experiments and modelling of NOx precursors release (NH3 and HCN) in fixed-bed biomass combustion conditions. Fuel 222, 529–537.

Barbaro, E., Zangrando, R., Moret, I., Barbante, C., Cescon, P., Gambaro, A., 2011. Free amino acids in atmospheric particulate matter of Venice, Italy. Atmos. Environ. 45, 5050–5057.

Barbaro, E., Zangrando, R., Vecchiato, M., Piazza, R., Cairns, W.R.L., Capodaglio, G., Barbante, C., Gambaro, A., 2015. Free amino acids in Antarctic aerosol: potential markers for the evolution and fate of marine aerosol. Atmos. Chem. Phys. 15, 5457–5469.

Barbaro, E., Feltracco, M., Cesari, D., Padoan, S., Zangrando, R., Contini, D., Barbante, C., Gambaro, A., 2019. Characterization of the water soluble fraction in ultrafine, fine, and coarse atmospheric aerosol. Sci. Total Environ. 658, 1423–1439.

Bond, T.C., Streets, D., Yarber, K., Nelson, S., 2004. A technology-based inventory of black and organic carbon emissions from combustion. J. Geophys. Res. Atmos. 109, D14203.

Casagrande, D.J., Gronli, K., Sutton, N., 1980. The distribution of sulfur and organic matter in various fractions of peat: origins of sulfur in coal. Geochem. Cosmochim. Acta 44, 25–32.

Chan, M.N., Choi, M.Y., Ng, N.L., Chan, C.K., 2005. Hygroscopicity of water-soluble organic compounds in atmospheric Aerosols: amino acids and biomass burning derived organic species. Environ. Sci. Technol. 39, 1555–1562.

Cheng, Y., Engling, G., He, K.B., Duan, F.K., Ma, Y.L., Du, Z.Y., Liu, J.M., Zheng, M., Weber, R.J., 2013. Biomass burning contribution to Beijing aerosol. Atmos. Chem. Phys. 13, 7765–7781.

Dauwe, B., Middelburg, J.J.J.L., 1999. Linking diagenetic alteration of amino acids and bulk organic matter reactivity. Oceanography 44, 1809–1814.

Deniro, M.J., Hastorf, C.A., 1985. Alteration of 15N14N and 13C12C ratios of plant matter during the initial stages of diagenesis: studies utilizing archaeological specimens from Peru. Geochem. Cosmochim. Acta 49, 97–115.

Deniro, M.J., Schoeninger, M.J., Hastorf, C.A., 1985. Effect of heating on the stable carbon and nitrogen isotope ratios of bone collagen. J. Archaeol. Sci. 12, 1–7.

Duan, X., Jiang, Y., Wang, B., Zhao, X., Shen, G., Cao, S., Huang, N., Qian, Y., Chen, Y., Wang, L., 2014. Household fuel use for cooking and heating in China: results from

the first Chinese environmental exposure-related human activity patterns survey (CEERHAPS). Appl. Energy 136, 692–703.

EPA, 2009. Integrated Science Assessment for Particulate Matter (Final Report). U. S. Environmental Protection Agency, Washington, DC.

Feng, J., Chan, C.K., Fang, M., Hu, M., He, L., Tang, X., 2006. Characteristics of organic matter in PM2.5 in Shanghai. Chemosphere 64, 1393–1400.

Fernandes, R., Meadows, J., Dreves, A., Nadeau, M.-J., Grootes, P., 2014. A preliminary study on the influence of cooking on the C and N isotopic composition of multiple organic fractions of fish (mackerel and haddock). J. Archaeol. Sci. 50, 153–159.

Fu, J.S., Hsu, N.C., Gao, Y., Huang, K., Li, C., Lin, N.H., Tsay, S.C., 2012. Evaluating the influences of biomass burning during 2006 BASE-ASIA: a regional chemical transport modeling. Atmos. Chem. Phys. 12, 3837–3855.

Ge, X., Wexler, A.S., Clegg, S.L., 2011. Atmospheric amines - Part I. A review. Atmos. Environ. 45, 524–546.

Harrison, R.M., Beddows, D.C.S., Hu, L., Yin, J., 2012. Comparison of methods for evaluation of wood smoke and estimation of UK ambient concentrations. Atmos. Chem. Phys. 12, 8271–8283.

Hennigan, C.J., Sullivan, A.P., Collett Jr., J.L., Robinson, A.L., 2010. Levoglucosan stability in biomass burning particles exposed to hydroxyl radicals. Geophys. Res. Lett. 37.

Ho, K.F., Ho, S.S.H., Huang, R.J., Liu, S.X., Cao, J.J., Zhang, T., Chuang, H.C., Chan, C.S., Hu, D., Tian, L., 2015. Characteristics of water-soluble organic nitrogen in fine particulate matter in the continental area of China. Atmos. Environ. 106, 252–261.

Huffman, J.A., Prenni, A.J., DeMott, P.J., Pöhlker, C., Mason, R.H., Robinson, N.H., Fröhlich-Nowoisky, J., Tobo, Y., Després, V.R., Garcia, E., Gochis, D.J., Harris, E., Müller-Germann, I., Ruzene, C., Schmer, B., Sinha, B., Day, D.A., Andreae, M.O., Jimenez, J.L., Gallagher, M., Kreidenweis, S.M., Bertram, A.K., Pöschl, U., 2013. High concentrations of biological aerosol particles and ice nuclei during and after rain. Atmos. Chem. Phys. 13, 6151–6164.

Joung, Y.S., Buie, C.R.J.N.C., 2015. Aerosol Generation by Raindrop Impact on Soil, vol. 6, 6083–6083.

Kelemen, S.R., Gorbaty, M.L., Kwiatek, P.J., 1994. Quantification of nitrogen forms in argonne premium coals. Energy Fuels 8, 896–906.

Kundu, S., Kawamura, K., Andreae, T.W., Hoffer, A., Andreae, M.O., 2010. Diurnal variation in the water-soluble inorganic ions, organic carbon and isotopic compositions of total carbon and nitrogen in biomass burning aerosols from the LBA-SMOCC campaign in Rondônia, Brazil. J. Aerosol Sci. 41, 118–133.

Kunwar, B., Kawamura, K., 2014. One-year observations of carbonaceous and nitrogenous components and major ions in the aerosols from subtropical Okinawa Island, an outflow region of Asian dusts. Atmos. Chem. Phys. 14, 1819–1836.

Li, W., Wang, C., Wang, H., Chen, J., Yuan, C., Li, T., Wang, W., Shen, H., Huang, Y., Wang, R., Wang, B., Zhang, Y., Chen, H., Chen, Y., Tang, J., Wang, X., Liu, J., Coveney, R.M., Tao, S., 2014. Distribution of atmospheric particulate matter (PM) in rural field, rural village and urban areas of northern China. Environ. Pollut. 185, 134–140.

Liu, J., Mauzerall, D.L., Chen, Q., Zhang, Q., Song, Y., Peng, W., Klimont, Z., Qiu, X., Zhang, S., Hu, M., Lin, W., Smith, K.R., Zhu, T., 2016. Air pollutant emissions from Chinese households: a major and underappreciated ambient pollution source. Proc. Natl. Acad. Sci. 113, 7756–7761.

Liu, F., Lai, S., Tong, H., Lakey, P.S.J., Shiraiwa, M., Weller, M.G., Pöschl, U., Kampf, C.J. J.A., 2017. Release of free amino acids upon oxidation of peptides and proteins by hydroxyl radicals. Anal. Bioanal. Chem. 409, 2411–2420.

Mace, K.A., Artaxo, P., Duce, R.A., 2003. Water-soluble organic nitrogen in Amazon Basin aerosols during the dry (biomass burning) and wet seasons. J. Geophys. Res. 108, D16.

Mandalakis, M., Apostolaki, M., Tziaras, T., Polymenakou, P., Stephanou, E.G., 2011. Free and combined amino acids in marine background atmospheric aerosols over the Eastern Mediterranean. Atmos. Environ. 45, 1003–1009.

Matos, J.T.V., Duarte, R.M.B.O., Duarte, A.C., 2016. Challenges in the identification and characterization of free amino acids and proteinaceous compounds in atmospheric aerosols: a critical review. Trends Anal. Chem. 75, 97–107.

McGregor, K.G., Anastasio, C., 2001. Chemistry of fog waters in California's Central Valley: 2. Photochemical transformations of amino acids and alkyl amines. Atmos. Environ. 35, 1091–1104.

Meier-Augenstein, W., 1999. Applied gas chromatography coupled to isotope ratio mass spectrometry. J. Chromatogr. A 842, 351–371.

Milne, P.J., Zika, R.G., 1993. Amino acid nitrogen in atmospheric aerosols: occurrence, sources and photochemical modification. J. Atmos. Chem. 16, 361–398.

Mopper, K., Zika, R.G.J.N., 1987. Free amino acids in marine rains: evidence for oxidation and potential role in nitrogen cycling. Nature 325, 246–249.

O'Leary, M.H., Urberg, M., Young, A.P., 1974. Nitrogen isotope effects on the papain-catalyzed hydrolysis of N-benzoyl-L-argininamide. Biochemistry 13, 2077–2081.

Qiu, X., Duan, L., Chai, F., Wang, S., Yu, Q., Wang, S., 2016. Deriving high-resolution emission inventory of open biomass burning in China based on satellite observations. Environ. Sci. Technol. 50, 11779–11786.

Ren, L., Bai, H., Yu, X., Wu, F., Yue, S., Ren, H., Li, L., Lai, S., Sun, Y., Wang, Z., 2018. Molecular composition and seasonal variation of amino acids in urban aerosols from Beijing, China. Atmos. Res. 203, 28–35.

Rui, D.A., Assunção, J.V.D., Pesquero, C.R., Bruns, R.E., Nóbrega, R.P., 2009. Emission of polycyclic aromatic hydrocarbons from gasohol and ethanol vehicles. Atmos. Environ. 43, 648–654.

Salma, I., Németh, Z., Weidinger, T., Maenhaut, W., Claeys, M., Molnár, M., Major, I., Ajtai, T., Utry, N., Bozóki, Z., 2017. Source apportionment of carbonaceous chemical species to fossil fuel combustion, biomass burning and biogenic emissions by a coupled radiocarbon–levoglucosan marker method. Atmos. Chem. Phys. 17, 13767–13781.

Samy, S., Robinson, J., Rumsey, I.C., Walker, J.T., Hays, M.D., Robinson, J., Rumsey, I.C., Hays, M.D., 2013. Speciation and trends of organic nitrogen in southeastern U.S. fine particulate matter (PM2.5). J. Geophys. Res.: Atmosphere 118, 1996–2006.

Scalabrin, E., Zangrando, R., Barbaro, E., Kehrwald, N.M., Gabrieli, J., Barbante, C., Gambaro, A., 2012. Amino acids in Arctic aerosols. Atmos. Chem. Phys. 12, 10453–10463.

Scheller, E., 2001. Amino acids in dew – origin and seasonal variation. Atmos. Environ. 35, 2179–2192.

Schimmelmann, A., Qi, H., Coplen, T.B., Brand, W.A., Fong, J., Meier-Augenstein, W., Kemp, H.F., Toman, B., Ackermann, A., Assonov, S., Aerts-Bijma, A.T., Brejcha, R., Chikaraishi, Y., Darwish, T., Elsner, M., Gehre, M., Geilmann, H., Gröning, M., Hélie, J.-F., Herrero-Martín, S., Meijer, H.A.J., Sauer, P.E., Sessions, A.L., Werner, R. A., 2016. Organic reference materials for hydrogen, carbon, and nitrogen stable isotope-ratio measurements: caffeines, n-alkanes, fatty acid methyl esters, glycines, l-valines, polyethylenes, and oils. Anal. Chem. 88, 4294–4302.

Simpson, I., Bol, R., Bull, I., Evershed, R., Petzke, K., Dockrill, S., 1999. Interpreting early land management through compound specific stable isotope analysis of archaeological soils. Rapid Commun. Mass Spectrom. 13, 1315–1319.

Song, T., Wang, S., Zhang, Y., Song, J., Liu, F., Fu, P., Shiraiwa, M., Xie, Z., Yue, D., Zhong, L., Zheng, J., Lai, S., 2017. Proteins and amino acids in fine particulate matter in rural Guangzhou, southern China: seasonal cycles, sources, and atmospheric processes. Environ. Sci. Technol. 51, 6773–6781.

Tao, S., Ru, M.Y., Du, W., Zhu, X., Zhong, Q.R., Li, B.G., Shen, G.F., Pan, X.L., Meng, W.J., Chen, Y.L., Shen, H.Z., Lin, N., Su, S., Zhuo, S.J., Huang, T.B., Xu, Y., Yun, X., Liu, J. F., Wang, X.L., Liu, W.X., Cheng, H.F., Zhu, D.Q., 2018. Quantifying the rural residential energy transition in China from 1992 to 2012 through a representative national survey. Nat. Energy 3, 567–573.

Tcherkez, G., 2011. Natural 15N/14N isotope composition in C3 leaves: are enzymatic isotope effects informative for predicting the 15N-abundance in key metabolites? Funct. Plant Biol. 38, 1–12.

Turekian, V.C., Macko, S., Ballentine, D., Swap, R.J., Garstang, M., 1998. Causes of bulk carbon and nitrogen isotopic fractionations in the products of vegetation burns: laboratory studies. Chem. Geol. 152, 181–192.

Vermeulen, I., Block, C., Vandecasteele, C., 2012. Estimation of fuel-nitrogen oxide emissions from the element composition of the solid or waste fuel. Fuel 94, 75–80.

Violaki, K., Mihalopoulos, N., 2010. Water-soluble organic nitrogen (WSON) in size-segregated atmospheric particles over the Eastern Mediterranean. Atmos. Environ. 44, 4339–4345.

Wang, Y., Zhuang, G., Xu, C., An, Z., 2007. The air pollution caused by the burning of fireworks during the lantern festival in Beijing. Atmos. Environ. 41, 417–431.

Wang, Y.Q., Zhang, X.Y., Draxler, R.R., 2009. TrajStat: GIS-based software that uses various trajectory statistical analysis methods to identify potential sources from long-term air pollution measurement data. Environmental Modelling & Software 24, 938–939.

Wedyan, M.A., Preston, M.R., 2008. The coupling of surface seawater organic nitrogen and the marine aerosol as inferred from enantiomer-specific amino acid analysis. Atmos. Environ. 42, 8698–8705.

Xiao, H.Y., Tang, C.G., Xiao, H.W., Liu, X.Y., Liu, C.Q., 2010. Mosses indicating atmospheric nitrogen deposition and sources in the Yangtze river drainage basin, China. J. Geophys. Res. Atmos. 115, D14.

Xiao, H.Y., Tang, C.G., Xiao, H.W., Liu, X.Y., Liu, C.Q., 2010. Stable sulphur and nitrogen isotopes of the moss Haplocladium microphyllum at urban, rural and forested sites. Atmos. Environ. 44, 4312–4317.

Xu, Y., Xiao, H., 2017. Concentrations and nitrogen isotope compositions of free amino acids in Pinus massoniana (Lamb.) needles of different ages as indicators of atmospheric nitrogen pollution. Atmos. Environ. 164, 348–359.

Yan, G., Kim, G., Kim, J., Jeong, Y.-S., Kim, Y.I., 2015. Dissolved total hydrolyzable enantiomeric amino acids in precipitation: implications on bacterial contributions to atmospheric organic matter. Geochem. Cosmochim. Acta 153, 1–14.

Zhang, Y., Schauer, J.J., Zhang, Y., Zeng, L., Wei, Y., Liu, Y., Shao, M., 2008. Characteristics of particulate carbon emissions from real-world Chinese coal combustion. Environ. Sci. Technol. 42, 5068–5073.

Zhang, Y., Yang, H., Pöschl, U., 2011. Analysis of nitrated proteins and tryptic peptides by HPLC-chip-MS/MS: site-specific quantification, nitration degree, and reactivity of tyrosine residues. Anal. Bioanal. Chem. 399, 459–471.

Zhang, Z., Wang, W., Cheng, M., Liu, S., Xu, J., He, Y., Meng, F., 2017. The contribution of residential coal combustion to PM2.5 pollution over China's Beijing-Tianjin-Hebei region in winter. Atmos. Environ. 159, 147–161.

Zhou, P., Xiong, S., Zhang, Y., Jiang, H., Chi, Y., Li, L., 2017. Study on the nitrogen transformation during the primary pyrolysis of sewage sludge by Py-GC/MS and Py-FTIR. Int. J. Hydrogen Energy 42, 18181–18188.

Zhu, R.-g., Xiao, H.-Y., Zhang, Z., Lai, Y., 2018. Compound-specific δ15N composition of free amino acids in moss as indicators of atmospheric nitrogen sources. Sci. Rep. 8, 14347.